Journal of Solid Mechanics Vol. 9, No. 2 (2017) pp. 225-238

Dynamic Instability of Visco-SWCNTs Conveying Pulsating Fluid Based on Sinusoidal Surface Couple Stress Theory

A. Ghorbanpour Arani [1, 2 *], R. Kolahchi [1], M. Jamali [1], M. Mosayyebi [1], I. Alinaghian[1]

[1] *Faculty of Mechanical Engineering, University of Kashan, Kashan, Iran*
[2] *Institute of Nanoscience & Nanotechnology, University of Kashan, Kashan, Iran*

Received 18 January 2017; accepted 23 March 2017

ABSTRACT

In this study, a realistic model for dynamic instability of embedded single-walled nanotubes (SWCNTs) conveying pulsating fluid is presented considering the viscoelastic property of the nanotubes using Kelvin–Voigt model. SWCNTs are placed in longitudinal magnetic fields and modeled by sinusoidal shear deformation beam theory (SSDBT) as well as modified couple stress theory. The effect of slip boundary condition and small size effect of nano flow are considered using Knudsen number. The Gurtin–Murdoch elasticity theory is applied for incorporation the surface stress effects. The surrounding elastic medium is described by a visco-Pasternak foundation model, which accounts for normal, transverse shear and damping loads. The motion equations are derived based on the Hamilton's principle. The differential quadrature method (DQM) in conjunction with Bolotin method is used in order to calculate the dynamic instability region (DIR) of visco-SWCNTs induced by pulsating fluid. The detailed parametric study is conducted, focusing on the combined effects of the nonlocal parameter, magnetic field, visco-Pasternak foundation, Knudsen number, surface stress and fluid velocity on the dynamic instability of SWCNTs. The results depict that increasing magnetic field and considering surface effect shift DIR to right. The results presented in this paper would be helpful in design and manufacturing of nano/micro mechanical systems.

Keywords : Dynamic instability; Pulsating fluid; Visco-SWCNTs; Surface effect; Modified couple stress theory.

1 INTRODUCTION

CARBON nanotubes (CNTs) are allotropes of carbon with a cylindrical nanostructure. Nanotubes have been constructed with length-to-diameter ratio of up to 132,000,000:1 [1]. significantly larger than for any other material. These cylindrical carbon molecules have unusual properties, which are valuable for nanotechnology, electronics, optics and other fields of materials science and technology. In particular, owing to their extraordinary thermal conductivity and mechanical and electrical properties, carbon nanotubes find applications as additives to various structural materials. For instance, nanotubes form a tiny portion of the material(s) in some (primarily carbon fiber) baseball bats, golf clubs, or car parts [2].

Nanotubes are members of the fullerene structural family. Their name is derived from their long, hollow structure with the walls formed by one-atom-thick sheets of carbon, called graphene. These sheets are rolled at specific and discrete ("chiral") angles, and the combination of the rolling angle and radius decides the nanotube

*Corresponding author. Tel.: +98 31 55912450; Fax: +98 31 55912424.
E-mail address: aghorban@kashanu.ac.ir (A.Ghorbanpour Arani).

properties; for example, whether the individual nanotube shell is a metal or semiconductor. Nanotubes are categorized as SWNTs and multi-walled nanotubes (MWNTs).

Sometimes, the classical theory cannot describe some phenomena of the material at atomic level. The classical (local) theory assumes that the stress at a defined point depends uniquely on the strain at the same point. But there are theories that are capable for considering small scale effects such as Eringen, couple stress, and modified couple stress and strain gradient. The modified couple stress has been used by many researchers in order to analyze size-dependent structures. For instance, Simşek and Reddy [3] investigated the bending and vibration of functionally graded micro beams using a new higher order beam theory and the modified couple stress theory. Wang et [4] presented the Size-dependent vibration analysis of three-dimensional cylindrical micro beams based on modified couple stress theory:A unified treatment.

In present, the mechanical behaviors of beams are being studied by applying various beam theories. It should be noted that the Euler-Bernoulli theory (EBT) is only applicable for slender beams and the shear deformation effect is not considered. The Timoshenko beam theory (TBT) accounts for the shear deformation effect for short beams by assuming a constant shear strain through the height of the beam. To avoid the use of shear correction factor, higher-order shear deformation theories were developed based on the assumption of the higher-order variation of axial displacement through the height of the beam such as sinusoidal shear deformation theory [5].

The vibration behavior of nano-tubes conveying fluid is one of the main problem of nano-tube structure, especially in targeted drug delivery systems. Kiani [6] studied the effects of small-scale parameter, inclination angle, speed and density of the fluid flow on the maximum dynamic amplitude factors of longitudinal and transverse displacements. Khodami Maraghi et al. [7] presented the nonlocal vibration and instability of embedded double-walled boron nitride nanotubes (DWBNNTs) conveying viscose fluid. They indicated that increasing flow velocity decreases system stability. As a matter of fact, the fluid velocity that is passing through the tube has not steady speed due to power systems. Therefore the flow inside the pipes and tubes becomes pulsative type and dynamic analysis must be considered in this situation. Based on nonlocal TBT, buckling analysis of a SWCNT embedded in an elastic medium was reported by Murmu and Pradhan [8]. Results show the dependency of critical dynamic load on nonlocal parameter and surrounding medium. Exact solution for nonlocal axial buckling of linear carbon nanotube hetero-junctions was presented by Ghorbanpour Arani et al. [9] based on Eringen's nonlocal theory. Ghorbanpour Arani et al. [9] carried out the nonlocal surface piezoelasticity theory for dynamic stability of DWBNNTs conveying viscose fluid based on different theories. In this study DIR of EBT, TBT and cylindrical shell theory are compared to each other. Numerical results indicate that neglecting the surface stress effects, the difference between DIR of three theories becomes remarkable. The stability analysis of a SWCNT conveying pulsating and viscous fluid with nonlocal effect was investigated by Liang and Su [10]. They showed that decrease of nonlocal parameter and increase of viscous parameter both increases the fundamental frequency and critical flow velocity.

The flow behavior at nano-scale is significantly different from those of macro/meso scales. Consequently, the assumption of no-slip boundary conditions between the flow and nanotube walls is no longer valid and a model should be presented to study the small-size effects of the flow field. Mirramezani et al. [11] showed that based on their result, they could have developed an innovative model for one dimensional coupled vibrations of CNTs conveying fluid using slip velocity of the fluid flow on the CNT walls as well as utilizing size-dependent continuum theories to consider the size effects of nano-flow and nano-structure. Kaviani and Mirdamadi [12] showed that considering the small-size effects of the flow field on the dynamic characteristics of CNTs conveying fluid is essential. They investigated wave propagation analysis of CNTs conveying fluid including slip boundary condition and strain/inertial gradient theory.

The effect of the surface free energy in nano scale structure is undeniable while in macro structures, the surface free energy is neglected in comparison with the bulk energy. Lee and Chang [13] carried out the surface effects on frequency analysis of nanotubes using nonlocal Timoshenko beam theory. Gheshlaghi and Hasheminejad [14] investigated the surface effects on nonlinear free vibration of nano beams. Malekzadeh and Shojaee [15] presented the surface and nonlocal effects on the nonlinear free vibration of non-uniform nano beams. They found that increase of the amplitude ratio causes reduction of the surface effects.

It has been proved that the CNTs deform when subjected to the magnetic field due to changes in their magnetic state. Kiani [16] investigated the vibration and instability of a SWCNT in a three-dimensional magnetic field. The obtained results reveal that the critical transverse magnetic field increases with the longitudinally induced magnetic field. Wang et al. [17] carried out the influences of longitudinal magnetic field on wave propagation in CNTs embedded in elastic matrix. The results obtained show that wave propagation in CNTs embedded in elastic matrix under longitudinal magnetic field appears in critical frequencies at which the velocity of wave propagation drops dramatically. Ghorbanpour Arani et al. [18] presented that the magnetic field is fundamentally an effective factor on increasing resonance frequency leading to stability of system.

In spite of many researches about behavior of CNTs using non-local elasticity theory, there are limited studies that consider non-local visco-elastic systems. Lei et al. [19] carried out the vibration of nonlocal Kelvin–Voigt viscoelastic damped Timoshenko beams. Ghorbanpour and Amir [20] investigated the electro-thermal vibration of visco-elastically coupled BNNT systems conveying fluid embedded on elastic foundation via strain gradient theory. Lei et al. [21] presented the Dynamic characteristics of damped viscoelastic nonlocal EBT.

However, to date, no report has been found in the literature on dynamic stability of viscoelastic SWCNTs conveying pulsating fluid based on surface sinusoidal modified couple stress theory. Motivated by these considerations, in order to improve optimum design of nanostructures, we aim to investigate pulsating fluid induced dynamic stability of visco-SWCNTs subjected to longitudinal magnetic field. The visco-SWCNTs are embedded in a realistic visco-Pasternak medium. Motion equations of system are derived using Hamilton's principal based on SSDBT and modified couple stress theory. The surface stress effects are also considered using Gurtin–Murdoch piezoelasticity theory. DQM and Bolotin method are applied for obtaining DIR of visco-SWCNTs. The influences of the nonlocal parameter, magnetic field, visco-Pasternak foundation, Knudsen number, surface stress and fluid velocity on the DIR of visco-SWCNTs are discussed in details.

2 BASIC EQUATIONS

A schematic of visco-SWCNT conveying pulsating fluid embedded in visco Pasternak foundation under longitudinal magnetic field is shown in Fig. 1.

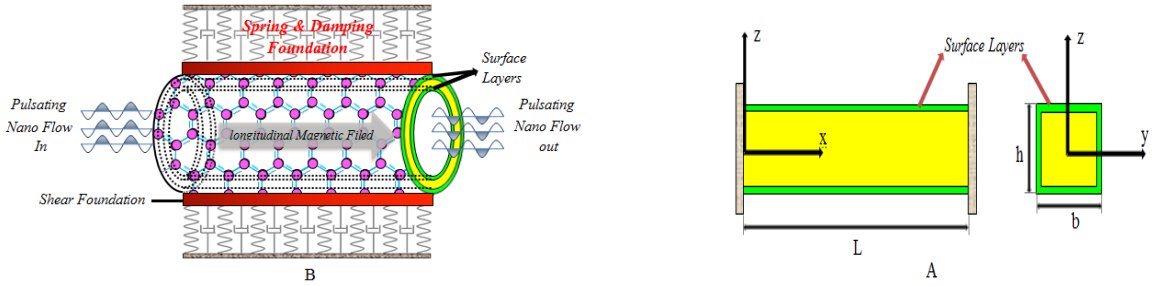

Fig.1
(a) A SWCNT conveying pulsating fluid embedded in visco Pasternak foundation under longitudinal magnetic field. (b) Schematic view of nanobeam with surface layers, coordinate system and geometrical parameters.

2.1 Viscoelastic SSDBT

The displacement fields of SWCNTs based on SSDBT can be described as [3]:

$$u_x(x,z,t) = u(x,t) - z\frac{\partial w(x,t)}{\partial x} + \Phi(z)\varphi(x,t), \tag{1a}$$

$$u_y(x,z,t) = 0, \tag{1b}$$

$$u_z(x,z,t) = w(x,t), \tag{1c}$$

$$\varphi(x,t) = \frac{\partial w(x,t)}{\partial x} - \phi(x,t), \tag{1d}$$

$$\Phi(z) = \frac{h}{\pi}\sin\left(\frac{\pi z}{h}\right), \tag{1e}$$

where u and w are the axial and the transverse displacement of any point on the neutral axis, t denotes time. φ and ϕ are the transverse shear strain of any point on the neutral axis and the total bending rotation of the cross-sections at any point on the neutral axis. $\Phi(z)$ is a function of Z, that characterizes the transverse shear and stress distribution along the thickness of the beam.

A material is usually thought of as just a solid or just a liquid. One that is visco-elastic may have both properties to some extent. According to Kelvin–Voigt [19] at real life, nano structure mechanical properties depend on the time variation. The Kelvin–Voigt model, consists of a Newtonian damper and Hookean elastic spring connected in parallel. This model represents, as the stress is released, the material gradually relaxes to its undeformed state. By considering this model, Young's modulus,E ,shear modulus,G and Young's modulus of surface, E_s are as follows:

$$\overline{E} = E\left(1+g\frac{\partial}{\partial t}\right), \tag{2a}$$

$$\overline{E_s} = E_s\left(1+g\frac{\partial}{\partial t}\right), \tag{2b}$$

$$\bar{G} = G\left(1+g\frac{\partial}{\partial t}\right), \tag{2c}$$

2.2 The modified couple stress theory

By considering the modified couple stress theory, the strain energy density is relate to the strain tensor and the curvature tensor. Thus the strain energy of bulk U_s^b in a deformed isotropic linear elastic material occupying region Ω is given by [4]:

$$U_s^b = \frac{1}{2}\int_{\Omega}(\sigma_{ij}\varepsilon_{ij} + m_{ij}\chi_{ij})dV \tag{3}$$

where ε_{ij} and χ_{ij} represent the strain and the symmetric rotation gradient tensors, respectively, which are defined by:

$$\varepsilon_{ij} = \frac{1}{2}\left(\frac{\partial u_j}{\partial x_i}+\frac{\partial u_i}{\partial x_j}\right) \tag{4}$$

$$\chi_{ij} = \frac{1}{2}\left(e_{ipq}\frac{\partial \varepsilon_{qj}}{\partial x_p}+e_{jpq}\frac{\partial \varepsilon_{qi}}{\partial x_p}\right) \tag{5}$$

where u_i and e_{ijk} are the displacement vector and the alternate tensor. The classical stress tensor, σ_{ij} the higher-order stresses, m_{ij} is given by:

$$\sigma_{ij} = \bar{E}\delta_{ij}\varepsilon_{mm} + 2\bar{G}\left(\varepsilon_{ij}-\frac{1}{3}\varepsilon_{mm}\delta_{ij}\right) \tag{6}$$

$$m_{ij} = 2l_0^2\bar{G}\chi_{ij} \tag{7}$$

where $\bar{E}$ and $\bar{G}$ are the bulk modulus and the shear modulus, l_0 is independent material length scale parameter.

2.3 Surface effect theory

The stress and deformation properties of nanostructures can be affected by surface effects. Actually at nano structure the surface to volume ratio is very large, therefore considering the effects of surface parameters is necessary.

The classical constitutive relation of the surface boundaries $(y=\pm b/2, z=\pm h/2)$ as given by Gurtin and Murdoch [22,23] and also the classical constitutive relations for the internal material of the beam $(-b/2 \prec y \prec b/2, -h/2 \prec z \prec h/2)$ as follows. Therefore, the constitutive equations for surface layers can be written as [24]:

$$\sigma^s_{\alpha\beta} = \tau_s \delta_{\alpha\beta} + (\lambda_s + \tau_s)\varepsilon_{\gamma\gamma}\delta_{\alpha\beta} + 2(\mu_s - \tau_s)\varepsilon_{\alpha\beta} + \tau_s u^s_{\alpha,\beta}, \tag{8a}$$

$$\sigma^s_{\alpha z} = \tau_s u^s_{z,\alpha}, \qquad (\alpha,\beta = x, y), \tag{8b}$$

where τ_s is the residual surface tension in the axial direction, μ_s and λ_s are the Lame parameters of surface layers.

The strain energy of surface, U^s_s is given by [25]:

$$U^s_s = \frac{1}{2}\int \left(\sigma^s_{\alpha\beta}\varepsilon_{\alpha\beta} + \sigma^s_{z\alpha}u^s_{z,\alpha}\right) dS. \tag{9}$$

where A, dS are the cross-sectional area of the beam and the line element, respectively.

2.4 Strain energy

The total strain energy is come to result by combining the modified couple stress theory and the surface effect theory as follows:

$$U_s = U^b_s + U^s_s \tag{10}$$

Total strain energy is came into result step by step as follows:
By substituting Eq. (1) into Eq. (4), the strain is

$$\varepsilon_x = \frac{\partial u}{\partial x} - z\frac{\partial^2 w}{\partial x^2} + \frac{h}{\pi}\left(\frac{\partial^2 w}{\partial x^2} - \frac{\partial \phi}{\partial x}\right) S(z) \tag{11a}$$

$$\varepsilon_{xz} = \frac{1}{2}\left(\frac{\partial w}{\partial x^2} - \phi\right) C(z), \tag{11b}$$

where

$$S(z) = \sin(\frac{\pi z}{h}), C(z) = \cos(\frac{\pi z}{h}) \tag{11c}$$

And by substituting Eq. (11) into Eq. (5) gives the symmetric rotation gradient tensor as:

$$\chi_{xy} = \chi_{yx} = -\frac{1}{2}\frac{\partial^2 w}{\partial x^2} + \frac{1}{4}\left(\frac{\partial^2 w}{\partial x^2} - \frac{\partial \phi}{\partial x}\right) C(z), \tag{12a}$$

$$\chi_{yz} = \chi_{zy} = \frac{1}{4}\frac{\pi}{h}\left(\phi - \frac{\partial w}{\partial x}\right)S(\mathrm{z}) , \tag{12b}$$

According to Gurtin–Murdoch model, σ_{zz} is not equal to zero on the inner and outer surfaces unlike classical beam theories. σ_{zz} varies linearly through the beam thickness and satisfies the balance conditions on the upper and lower surfaces and its defined as follows [24,26]:

$$\begin{aligned}\sigma_{zz} &= \frac{1}{2}\left(\sigma_z^+ + \sigma_z^-\right) + \frac{z}{h}\left(\sigma_z^+ - \sigma_z^-\right) \\ &= \frac{1}{2}\left(\frac{\partial \sigma_{xz}^s}{\partial x} - \rho_s \frac{\partial^2 w}{\partial t^2}\right)^+ + \frac{1}{2}\left(\frac{\partial \sigma_{xz}^s}{\partial x} - \rho_s \frac{\partial^2 w}{\partial t^2}\right)^- + \frac{z}{h}\left(\frac{\partial \sigma_{xz}^s}{\partial x} - \rho_s \frac{\partial^2 w}{\partial t^2}\right)^+ - \frac{z}{h}\left(\frac{\partial \sigma_{xz}^s}{\partial x} - \rho_s \frac{\partial^2 w}{\partial t^2}\right)^- ,\end{aligned} \tag{13a}$$

where ρ_s is mass density of surface layers and by substituting Eq. (8b) into Eq. (13a) yields the following relation as:

$$\sigma_{zz} = \frac{2z}{h}\left(\tau_s \frac{\partial^2 w}{\partial x^2} - \rho_s \frac{\partial^2 w}{\partial t^2}\right). \tag{13b}$$

Hence, by using Eqs. (13b), (11), (6) and (2) the stresses of bulk are

$$\sigma_x = \bar{E}\left\{\frac{\partial u}{\partial x} - z\frac{\partial^2 w}{\partial x^2} + \frac{h}{\pi}\left(\frac{\partial^2 w}{\partial x^2} - \frac{\partial \phi}{\partial x}\right)S(z)\right\} + v\,\sigma_{zz} \tag{13c}$$

$$\sigma_{xz} = \bar{G}\left\{\frac{1}{2}\left(\frac{\partial w}{\partial x} - \phi\right)C(z)\right\} \tag{13d}$$

where v is the poisson ratio of nanotube. Moreover, Using Eqs. (8), the surface stresses are derived as follows:

$$\sigma_x^s = \tau_s + \bar{E}_s \varepsilon_x \tag{14a}$$

$$\sigma_{xz}^s = \tau_s \frac{\partial w}{\partial x} \tag{14b}$$

where $\bar{E}_s = \left(1 + g\frac{\partial}{\partial t}\right)\left(2\mu_s + \lambda_s\right)$. By considering Eq. (2) and substituting Eq. (12) into Eq. (7) the higher-order stresses m_{ij} are

$$m_{xy} = m_{yx} = 2l_0^2\bar{G}\left\{-\frac{1}{2}\frac{\partial^2 w}{\partial x^2} + \frac{1}{4}\left(\frac{\partial^2 w}{\partial x^2} - \frac{\partial \phi}{\partial x}\right)C(z)\right\} \tag{15a}$$

$$m_{yz} = m_{zy} = 2l_0^2\bar{G}\left\{\frac{1}{4}\frac{\pi}{h}\left(\phi - \frac{\partial w}{\partial x}\right)S(z)\right\} \tag{15b}$$

Substituting Eqs. (11)- (15) into Eq. (10), leads to

$$U_s = \frac{1}{2}\int_0^L \int_0^L \left\{ \zeta_1 \left(\frac{\partial u}{\partial x}\right)^2 + \zeta_2 \left(\frac{\partial^2 w}{\partial x^2}\right)^2 + \zeta_3 \left(\frac{\partial w}{\partial x}\right)^2 + \zeta_4 \left(\frac{\partial^2 w}{\partial x^2}\frac{\partial u}{\partial x}\right) + \zeta_5 \left(\frac{\partial^2 w}{\partial x^2}\frac{\partial \phi}{\partial x}\right) + \zeta_6 \left(\phi \frac{\partial w}{\partial x}\right) + \zeta_7 \left(\frac{\partial \phi}{\partial x}\right)^2 \right.$$
$$\left. + \zeta_8 \left(\frac{\partial \phi}{\partial x}\frac{\partial u}{\partial x}\right) + \zeta_9 (\phi)^2 + \zeta_{10}\frac{\partial u}{\partial x} + \zeta_{11}\frac{\partial^2 w}{\partial x^2} + \zeta_{12}\frac{\partial \phi}{\partial x} + \zeta_{13}\left(\frac{\partial^2 w}{\partial x^2}\frac{\partial^2 w}{\partial t^2}\right) + \zeta_{14}\left(\frac{\partial \phi}{\partial x}\frac{\partial^2 w}{\partial t^2}\right) \right\} dx \tag{16a}$$

where

$$\begin{aligned}
&\zeta_1 = \bar{E}A + \bar{E}_s S, \\
&\zeta_2 = -l_0^2\left(\bar{G}T_0\right) + l_0^2\left(\frac{1}{4}\bar{G}O\right) + l_0^2\left(\bar{G}A\right) + \bar{E}I + \bar{E}I_s - 2\frac{h}{\pi}\left(\bar{E}P + \bar{E}_s P_1\right) + \frac{h^2}{\pi^2}\left(\bar{E}L + \bar{E}_s L_s\right) - 2\frac{\nu\,\tau_s I}{h} + 2\frac{\nu\,\tau_s P_1}{\pi}, \\
&\zeta_3 = \frac{1}{4}\frac{l_0^2 \bar{G}L\pi^2}{h^2} + \bar{G}O + \tau_s T_0, \zeta_4 = 2\frac{h}{\pi}\left(\bar{E}P_0 + \bar{E}_s P_0\right), \\
&\zeta_5 = -l_0^2\left(\frac{1}{2}\bar{G}O\right) + l_0^2\left(\bar{G}T_0\right) - 2\frac{h^2}{\pi^2}\left(\bar{E}L + \bar{E}_s L_s\right) + 2\frac{h}{\pi}\left(\bar{E}P_1 + \bar{E}_s P_1\right) - 2\frac{\nu\,\tau_s P_1}{\pi} \\
&\zeta_6 = -\frac{1}{2}\frac{l_0^2 \bar{G}L\pi^2}{h^2} - 2\bar{G}O - \tau_s T_0, \zeta_7 = l_0^2\left(\frac{1}{4}\bar{G}O\right) + \frac{h^2}{\pi^2}\left(\bar{E}L + \bar{E}_s L_s\right), \zeta_8 = -2\frac{h}{\pi}\left(\bar{E}P_0 + \bar{E}_s P_0\right), \\
&\zeta_9 = \frac{1}{4}\frac{l_0^2 \bar{G}L\pi^2}{h^2} + \bar{G}O, \zeta_{10} = \tau_s S, \zeta_{11} = \frac{\tau_s h P_0}{\pi}, \zeta_{12} = \frac{\tau_s h P_0}{\pi}, \zeta_{13} = 2\frac{\nu\,\rho_s I}{h} - 2\frac{\nu\,\rho_s P_1}{\pi}, \zeta_{14} = 2\frac{\nu\,\rho_s P_1}{\pi}
\end{aligned} \tag{16b}$$

where the following integrals are defined

$$\begin{pmatrix} (A, I, P_0, P_1, T_0, L, O) \\ (S, I_s, P_0, P_1, T_0, L_s, O_s) \end{pmatrix} = \int_{A,S} \begin{pmatrix} \xi & 0 \\ 0 & \xi \end{pmatrix} \begin{pmatrix} dA \\ dS \end{pmatrix} \tag{16c}$$

where

$$\xi = \left(1, z^2, S(z), S(z), zC(z), (S(z))^2, (C(z))^2\right) \tag{16d}$$

The total kinetic energy nanotubes can be expressed as:

$$k_{tube} = \frac{1}{2}\rho_t \int_0^L \left\{ \int_A \left[\left(\frac{\partial \tilde{u}_x}{\partial t}\right)^2 + \left(\frac{\partial \tilde{u}_z}{\partial t}\right)^2 \right] dA \right\} dx \tag{17}$$

where ρ_t is the mass density of nanotubes.

2.5 Longitudinal magnetic field and elastic medium

Maxwell's equation are given by [17]:

$$\vec{J} = \nabla \times \vec{h}, \nabla \times e = -\eta\left(\frac{\partial h}{\partial t}\right), \nabla . \vec{h} = 0, e = -\eta\left(\frac{\partial D}{\partial t} \times \vec{H}\right), \vec{h} = \nabla \times (\vec{D} \times \vec{H}) \tag{18}$$

where, $\vec{J}, e, \eta$ and h represent the current density, strength vectors of electric field, is the magnetic field permeability and disturbing vectors of magnetic field respectively. $\vec{D} = (u_x, u_y, u_z)$ is the displacement vector and $\vec{H} = (H_x, 0, 0)$ is the magnetic field vector.

By using Eq. (18) $\vec{h}$ and $\vec{J}$ are describe:

$$\vec{h} = \nabla \times \left(D \times \vec{H} \right) = H_x \frac{\partial w}{\partial x} k \tag{19}$$

$$\vec{j} = \vec{J} = \nabla \times \vec{h} = -H_x \frac{\partial^2 w}{\partial x^2} \tag{20}$$

The Lorentz force in three directions is:

$$\vec{f} = (f_x, f_y, f_z) = \eta(\vec{J} \times \vec{H}) \tag{21}$$

Introducing Eq. (20) to Eq. (21), the Lorentzian forces are obtained as:

$$\vec{f} = (f_x, f_y, f_z) = \left(0, 0, \eta H_x^2 \frac{\partial^2 w}{\partial x^2} \right) \tag{22}$$

Eventually, Lorentz work is written as [16]:

$$W_{lorentz} = \int_0^L (f_z w) dx \tag{23}$$

The external work due to visco-Pasternak foundation is written as:

$$W_{visco-pasternak} = \int_0^L (-K_w w + G_P \nabla^2 w) w dx + \int_0^L C_d \frac{\partial w}{\partial t} dx \tag{24}$$

where K_w, C_d and G_P Winkler's spring modulus, damper and Pasternak's shear modulus of elastic medium, respectively.

2.6 Virtual work of pulsating nano-flow

According to the reference [11], the viscosity parameter could not appear in the fluid–structure interaction(FSI) equation. So the force exerted due to the fluid flow on the nanotube can be obtained as follows:

$$F_f = A_f \frac{\partial p_r}{\partial r} - \mu_0 A_f \left[\frac{\partial^3 W}{\partial x^2 \partial t} + V_f \frac{\partial^3 W}{\partial x^3} \right] = -\rho A_f \left[\frac{\partial^2 W}{\partial t^2} + 2V_f \frac{\partial^2 W}{\partial x \partial t} + V_f^2 \frac{\partial^2 W}{\partial x^2} \right] \tag{25}$$

where F_f is the exerted force by fluid to the nanotube. A_f, ρ, V_f and μ denote the cross sectional area of the internal fluid, the fluid density, the velocity of the fluid flow in the longitudinal direction on the CNT wall and the viscosity of the flowing fluid, respectively.

Based on Kn, four flow regimes may be identified and for $(i.e. 0.01 \prec Kn \prec 0.1)$ the slip flow regime could be considered. For CNTs conveying fluid, the Kn may be larger than 10^{-2}; consequently, the assumption of no-slip

boundary condition should be no longer valid and the fluid slip velocity should be modified. The slip velocity is presented as follows [11]:

$$V_{avg,slip} = \frac{\gamma}{1+\gamma} V_{avg\,(no-slip)} \tag{26a}$$

where

$$\gamma = 4\left(\frac{2-\sigma_v}{\sigma_v}\right)\left(\frac{Kn}{1+Kn}\right) \tag{26b}$$

Here σ_v is tangential moment accommodation coefficient and is considered to be 0.7 for most practical purpose.

The case of pulsating internal flow is assumed harmonically fluctuating ,as follows [10]:

$$V_f = V_{avg,(no-slip)} = V_0\left(1+\alpha\cos(\omega t)\right) \tag{27}$$

where V_0 is the mean flow velocity, α is the amplitude of the harmonic fluctuation (assumed small) and ω its frequency.

The total virtual work of pulsating nano-flow is

$$W_{fluid} = \int_0^l F_f w dx = \int_0^l \left\{-\rho A_f \left[\frac{\partial^2 w}{\partial t^2} + 2U_f \frac{\partial^2 w}{\partial x\,\partial t} + U_f^2 \frac{\partial^2 w}{\partial x^2}\right]\right\} w dx \tag{28}$$

It is noticed that $U_f = \frac{\gamma}{1+\gamma} \times V_f$ in the governing equations.

2.7 Hamilton's principle

The energy method is applied to derive equations of motion, in this study. Total potential energy Π , is given by:

$$\Pi = U_s - (K + W) \tag{29}$$

U_s , K and W denote total strain energy, total kinetic energy and the total external work in SWCNTs system. Hamilton's principle is used to derive the motion equations of embedded SWCNTs conveying pulsating viscose fluid as follows:

$$\int_{t_0}^{t_1} \left[\delta U_s - (\delta K_{nanotube} + \delta W_{fluid} + \delta W_{florentz} + \delta W_{visco-pasternak})\right] = 0 \tag{30}$$

According to this principal, the motion equations are obtained as follows:

$$\delta u: \quad -2\zeta_1 \frac{\partial^2 u}{\partial x^2} - \zeta_4 \frac{\partial^3 w}{\partial x^3} - \zeta_8 \frac{\partial^2 \phi}{\partial x^2} + \rho_t A \frac{\partial^2 u}{\partial t^2} + \frac{\rho_t h P_0}{\pi} \frac{\partial^3 w}{\partial x\,\partial t^2} - \frac{\rho_t h P_0}{\pi} \frac{\partial^2 \phi}{\partial t^2}, \tag{31}$$

$$\begin{aligned}\delta w:\ & 2\zeta_2\frac{\partial^4 w}{\partial x^4}+\zeta_5\frac{\partial^3\phi}{\partial x^3}-2\zeta_3\frac{\partial^2 w}{\partial x^2}-\zeta_6\frac{\partial\phi}{\partial x}+\zeta_4\frac{\partial^3 u}{\partial x^3}+2\zeta_{13}\frac{\partial^4 w}{\partial x^2\partial t^2}+\zeta_{14}\frac{\partial^3\phi}{\partial x\,\partial t^2}-\frac{\rho_t hP_1}{\pi}\frac{\partial^3\phi}{\partial x\,\partial t^2}\\ & -\frac{\rho_t h^2 L}{\pi^2}\frac{\partial^4 w}{\partial x^2\partial t^2}+\frac{\rho_t h^2 L}{\pi^2}\frac{\partial^3\phi}{\partial x\,\partial t^2}-I\rho_t\frac{\partial^4 w}{\partial x^2\partial t^2}+\rho_t A\frac{\partial^2 w}{\partial t^2}-\frac{\rho_t hP_0}{\pi}\frac{\partial^3 u}{\partial x\,\partial t^2}+2\frac{\rho_t hP_1}{\pi}\frac{\partial^4 w}{\partial x^2\partial t^2}\\ & -2\tau_s(h+b)\frac{\partial^2 w}{\partial x^2}-f_z+\rho A_f\frac{\partial^2 w}{\partial t^2}+2\rho A_f U_f\frac{\partial^2 w}{\partial x\,\partial t}+\rho A_f U_f^2\frac{\partial^2 w}{\partial x^2}-G_p\nabla^2 w+K_w w+c_d\frac{\partial w}{\partial t}\end{aligned} \tag{32}$$

$$\begin{aligned}\delta\phi:\ & -\zeta_5\frac{\partial^3 w}{\partial x^3}+\zeta_6\frac{\partial w}{\partial x}+2\zeta_9\phi-2\zeta_7\frac{\partial^2\phi}{\partial x^2}-\zeta_8\frac{\partial^2 u}{\partial x^2}-\zeta_{14}\frac{\partial^3 w}{\partial x\,\partial t^2}-\frac{\rho_t hP_0}{\pi}\frac{\partial^2 u}{\partial t^2}\\ & +\frac{\rho_t hP_1}{\pi}\frac{\partial^3 w}{\partial x\,\partial t^2}-\frac{\rho_t h^2 L}{\pi^2}\frac{\partial^3 w}{\partial x\,\partial t^2}+\frac{\rho_t h^2 L}{\pi^2}\frac{\partial^2\phi}{\partial t^2}.\end{aligned} \tag{33}$$

Furthermore, the essential boundary conditions at $x=0$ and $x=L$ may be obtained as:

$$\begin{aligned}&\frac{\partial^2\delta w}{\partial x^2}=0\ ,\ \frac{\partial\delta w}{\partial x}=0\ ,\ \delta w=0\ ,\\ &\frac{\partial\delta\phi}{\partial x}=0\ ,\ \delta\phi=0\ ,\\ &\frac{\partial\delta u}{\partial x}=0\ ,\ \delta u=0\ .\end{aligned} \tag{34}$$

3 SOLLUTION PROCEDURE

3.1 DQM

DQM is employed in this section which in essence approximates the partial derivative of a function, with respect to a spatial variable at a given discrete point, as a weighted linear sum of the function values at all discrete points chosen in the solution domain of the spatial variable [7, 18]. Let F be a function representing u_1,u_2,w_1,w_2 and ϕ_1,ϕ_2 with respect to variable x in the domain of $(0\prec x\prec L)$ having N_x grid points along these variable. The n^{th}-order partial derivative of $F(x)$ with respect to x may be expressed discretely as:

$$\frac{d^n F(x_i)}{dx^n}=\sum_{k=1}^{N_x}A_{ik}^{(n)}F(x_k)\qquad n=1,...,N_x-1 \tag{35}$$

where $A_{ik}^{(n)}$ is the weighting coefficient, whose recursive formula are described in [7]. Chebyshev polynomials [7, 18] was used to determine the positions of the grid points.

Combining all the motion equations along with the corresponding boundary conditions using DQM and rewritten them in matrix form yields

$$[M]\{\ddot{d}\}+\left([C]+(V_0+V_0\alpha\cos(\omega t))[C]^f\right)\{\ddot{d}\}+\left([K]+(V_0+V_0\alpha\cos(\omega t))^2[K]^f\right)\{d\}=0 \tag{36}$$

where $[M][C]$ and $[K]$ are the mass, damping and stiffness matrixes, respectively; $[C]^f$ and $[K]^f$ are the respectively, damping and stiffness matrixes related to pulsating fluid; $\{d\}$ is the displacement vector $(i.e.\{d\}=\{u_i,v_i,w_i\}\ \ i=1,2)$.

3.2 Bolotin method

In order to determinate the DIR of visco-SWCNTs, the method suggested by Bolotin [27] is applied. Hence, the components of $\{d\}$ can be written in the Fourier series with period $2T$ as:

$$\{d\} = \sum_{k=1,3,\ldots}^{\infty} \left[\{a\}_k \sin\frac{k\omega t}{2} + \{b\}_k \cos\frac{k\omega t}{2} \right] \tag{37}$$

According to this method, The first instability region is usually the most important in studies of structures. It is due to the fact that the first DIR is wider that other DIRs and structural damping in higher regions becomes neutralize [28]. Substituting Eq. (37) into Eq. (36) and setting the coefficients of each sine and cosine as well as the sum of the constant terms to zero, yields

$$\left| \left([K] + \left(1 \pm \alpha + \frac{\alpha^2}{2} \right) [K]^f \right) + \left(\pm [C] \frac{\omega}{2} + \left(\frac{\alpha\omega}{4} \pm \frac{\omega}{2} \right) [C]^f \right) - [M] \frac{\omega^2}{4} \right| = 0 \tag{38}$$

Solving the above equation based on eigenvalue problem, the variation of ω with respect to α can be plotted as DIR.

4 RESULTS AND DISCUSSION

In this approach, the effects of nonlocal parameter, magnetic field, visco-Pasternak foundation, Knudsen number, surface stress and fluid velocity on the DIR of simply supported visco-SWCNTs are investigated. The material properties of the SWCNTs related to bulk are: Young's modulus of $E = 1\ Tpa$, Poisson's ratio of $v = 0.27$, density of $\rho = 2300\,Kg/m^3$ and thickness of $h = 0.34nm$ [29]. Generally, the surface material properties can be calculated by atomic simulations. However, the material properties of the SWCNTs related to surface are: surface Young's modulus of, $E^s = 35.3\,N/m$ and residual surface stress of, $\tau^s = 0.31\,N/m$ [29].

Fig. 2 illustrates the effect of various surrounding foundation on the dimensionless pulsation frequency. Four different elastic medium are considered namely as visco-Pasternak $(i.e. K_w = 1\times10^{17}, G_p = 4, C_d = 10)$, Pasternak $(i.e. K_w = 1\times10^{17}, G_p = 4, C_d = 0)$, visco-Winkler $(i.e. K_w = 1\times10^{17}, G_p = 0, C_d = 10)$ and Winkler $(i.e. K_w = 1\times10^{17}, G_p = 0, C_d = 0)$ mediums. It is understood that elastic foundation increases the dimensionless pulsation frequency and DIR shifts to right. It is due to the fact that putting SWCNT in an elastic medium makes the system more stable and stiffer. It is also concluded that the DIR of Pasternak or visco-Pasternak model is higher than Winkler or visco-Winkler one. It is because Pasternak model considers not only the normal stresses but also the transverse shear deformation and continuity among the spring elements. Furthermore, the DIR predicted by visco-Pasternak and visco-Winkler mediums is lower than Pasternak and Winkler models, respectively.

Fig. 3 shows the dimensionless pulsation frequency with respect to the dimensionless pulsation amplitude for different values of fluid velocities and Knudsen numbers. Increasing the fluid velocity generates compressive axial load, thus the dimensionless pulsation frequency and DIR will decrease. As we know when the Knudsen- number increases, the mean free path of liquid molecules increases and results in lower stiffness, so by enhancing *Kn*, DIR and the dimensionless pulsation frequency shift to left and decrease.

Fig. 4 depicts the surface stress effect and magnetic field intensity on the dimensionless pulsation frequency with respect to the dimensionless pulsation amplitude. In this figure, SE and WSE means that with surface effect and without surface effect, respectively. It is obvious that increasing magnetic field intensity and considering surface effect cause the DIR and dimensionless pulsation frequency shifts to right and increases, respectively. This is due to the fact that considering surface effect and increment magnetic field intensity make the system more stable.

Fig.5 demonstrates variations of the dimensionless pulsation frequency versus the dimensionless pulsation amplitude for different nonlocal parameter. It can be observed that increment of nonlocal parameter in modified couple stress theory makes the DIR and dimensionless pulsation frequency shift to right and increase. This is because the modified couple stress theory expresses the one additional rotation gradient tensor.

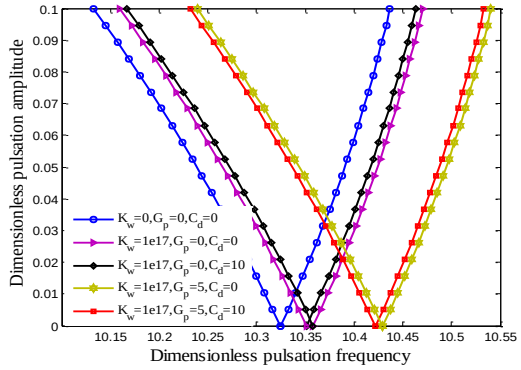

Fig.2
Dimensionless pulsation amplitude versus dimensionless pulsation frequency for different elastic medium.

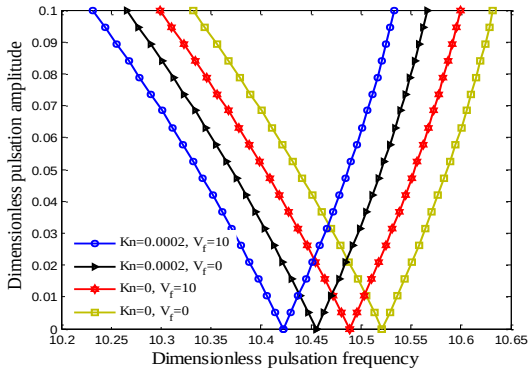

Fig.3
Dimensionless pulsation amplitude versus dimensionless pulsation frequency for different values of Knudsen number and fluid velocities.

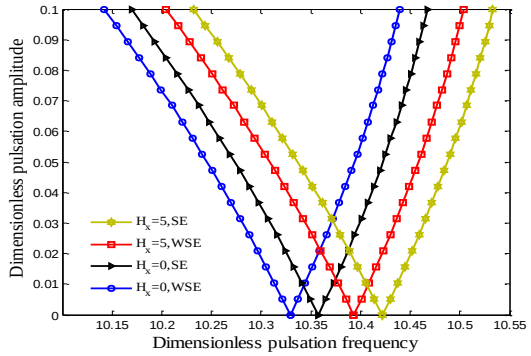

Fig.4
Dimensionless pulsation amplitude versus dimensionless pulsation frequency for different values of magnetic field and surface effect parameters.

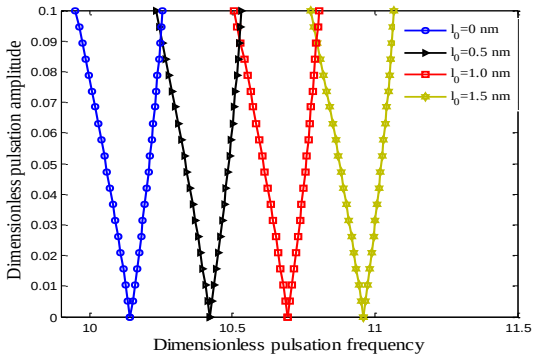

Fig.5
Dimensionless pulsation amplitude versus dimensionless pulsation frequency for different values of nonlocal parameter.

5 CONCLUSIONS

Dynamic responses of SWCNTs have applications in designing many NEMS/MEMS devices such as sensors, actuators, fluid storage and solar cell. However, dynamic stability of SWCNTs conveying pulsating fluid subjected to longitudinal magnetic field was studied in this paper. This work furthers previous studies in four aspects; considering fluid as pulsating with small size effect of nano flow, assuming SWCNTs as viscoelastic based on Kelvin-Voigt model, modeling of visco-SWCNTs using SSDBT and modified couple stress theory, applying Gurtin–Murdoch theory for surface stress effects. DIR of the visco-SWCNT was obtained using Bolotin method in conjunction with DQM. The effects of nonlocal parameter, magnetic field, visco-Pasternak foundation, Knudsen number, surface stress and fluid velocity were shown in dynamic response of system. The following conclusions may be made from the results:

1. Regarding fluid flow effects, it has been concluded that the fluid flow is basically an effective factor on decreasing DIR of visco-SWCNTs.
2. The DIR of visco-SWCNTs was strongly dependent on the imposed magnetic field so that increasing the imposed magnetic field significantly increases the DIR of visco-SWCNTs. In this case the DIR of the system can be controlled by imposing magnetic field and the visco-SWCNTs can behave as an actuator.
3. The DIR predicted by the modified couple stress theory was higher than the classical one.
4. By enhancing Kn, DIR and the dimensionless pulsation frequency shift to left and decrease.
5. Considering surface effect, it causes the DIR and dimensionless pulsation frequency shift to right and increase.

ACKNOWLEDGMENTS

The author would like to thank the reviewers for their comments and suggestions to improve the clarity of this article. The authors are grateful to University of Kashan for supporting this work by Grant No. 574600/26.

REFERENCES

[1] Wang X., Li Q., Xie J., Jin Z., Wang J., Li Y., Jiang K., Fan S., 2009, Fabrication of ultralong and electrically uniform single-walled carbon nanotubes on clean substrates, *Nano Letters* **9**: 3137-3141.

[2] Wong M., Gullapalli S., 2011, *Nanotechnology: A Guide to Nano-Objects*, Chemical Engineering Progress.

[3] Şimşek M., Reddy J.N., 2013, Bending and vibration of functionally graded microbeams using a new higher order beam theory and the modified couple stress theory, *International Journal of Engineering Science* **64**: 37-53.

[4] Wang L., Xu Y.Y., Ni Q., 2013, Size-dependent vibration analysis of three-dimensional cylindrical microbeams based on modified couple stress theory: A unified treatment, *International Journal of Engineering Science* **68**: 1-10.

[5] Thai H-T., Vo T.P., 2012, A nonlocal sinusoidal shear deformation beam theory with application to bending, buckling, and vibration of nanobeams, *International Journal of Engineering Science* **54**: 58-66.

[6] Kiani K., 2013, Vibration behavior of simply supported inclined single-walled carbon nanotubes conveying viscous fluids flow using nonlocal Rayleigh beam model, *Applied Mathematical Modelling* **37**: 1836-1850.

[7] Khodami Maraghi Z., Ghorbanpour Arani A., Kolahchi R., Amir S., Bagheri M.R., 2013, Nonlocal vibration and instability of embedded DWBNNT conveying viscose fluid, *Composites Part B: Engineering* **45**: 423-432.

[8] Murmu T., Pradhan S.C., 2009, Buckling analysis of a single-walled carbon nanotube embedded in an elastic medium based on nonlocal elasticity and Timoshenko beam theory and using DQM, *Physica E: Low-Dimensional Systems and Nanostructures* **41**: 1232-1239.

[9] Ghorbanpour Arani A., Kolahchi R., Hashemian M., 2014, Nonlocal surface piezoelasticity theory for dynamic stability of double-walled boron nitride nanotube conveying viscose fluid based on different theories, *Proceedings of the Institution of Mechanical Engineers, Part C: Journal of Mechanical Engineering Science*.

[10] Liang F., Su Y., 2013, Stability analysis of a single-walled carbon nanotube conveying pulsating and viscous fluid with nonlocal effect, *Applied Mathematical Modelling* **37**: 6821-6828.

[11] Mirramezani M., Mirdamadi H.R., Ghayour M., 2013, Innovative coupled fluid–structure interaction model for carbon nano-tubes conveying fluid by considering the size effects of nano-flow and nano-structure, *Computational Materials Science* **77**: 161-171.

[12] Kaviani F., Mirdamadi H.R., 2013, Wave propagation analysis of carbon nano-tube conveying fluid including slip boundary condition and strain/inertial gradient theory, *Computers & Structures* **116**: 75-87.

[13] Lee H.L., Chang W.J., 2010, Surface effects on frequency analysis of nanotubes using nonlocal Timoshenko beam theory, *Journal of Applied Physics* **108**: 093503.
[14] Gheshlaghi B., Hasheminejad S.M., 2011, Surface effects on nonlinear free vibration of nanobeams, *Composites Part B: Engineering* **42**: 934-937.
[15] Malekzadeh P., Shojaee M., 2013, Surface and nonlocal effects on the nonlinear free vibration of non-uniform nanobeams, *Composites Part B: Engineering* **52**: 84-92.
[16] Kiani K., 2014, Vibration and instability of a single-walled carbon nanotube in a three-dimensional magnetic field, *Journal of Physics and Chemistry of Solids* **75**: 15-22.
[17] Wang H., Dong K., Men F., Yan Y.J., Wang X., 2010, Influences of longitudinal magnetic field on wave propagation in carbon nanotubes embedded in elastic matrix, *Applied Mathematical Modelling* **34**: 878-889.
[18] Ghorbanpour Arani A., Amir S., Dashti P., Yousefi M., 2014, Flow-induced vibration of double bonded visco-CNTs under magnetic fields considering surface effect, *Computational Materials Science* **86**: 144-154.
[19] Lei Y., Adhikari S., Friswell M.I., 2013, Vibration of nonlocal Kelvin–Voigt viscoelastic damped Timoshenko beams, *International Journal of Engineering Science* **66**: 1-13.
[20] Ghorbanpour Arani A., Amir S., 2013, Electro-thermal vibration of visco-elastically coupled BNNT systems conveying fluid embedded on elastic foundation via strain gradient theory, *Physica B: Condensed Matter* **419**: 1-6.
[21] Lei Y., Murmu T., Adhikari S., Friswell M.I., 2013, Dynamic characteristics of damped viscoelastic nonlocal Euler–Bernoulli beams, *European Journal of Mechanics - A/Solids* **42**: 125-136.
[22] Gurtin M., Ian Murdoch A., 1975, A continuum theory of elastic material surfaces, *Archive for Rational Mechanics and Analysis* **57**: 291-323.
[23] Gurtin M., Ian Murdoch A., 1978, Surface stress in solids, *International Journal of Solids and Structures* **14**: 431-440.
[24] Ansari R., Ashrafi M.A., Pourashraf T., Sahmani S., 2015, Vibration and buckling characteristics of functionally graded nanoplates subjected to thermal loading based on surface elasticity theory, *Acta Astronautica* **109**: 42-51.
[25] Shaat M., Mohamed S.A., 2014, Nonlinear-electrostatic analysis of micro-actuated beams based on couple stress and surface elasticity theories, *International Journal of Mechanical Sciences* **84**: 208-217.
[26] Ansari R., Sahmani S., 2011, Bending behavior and buckling of nanobeams including surface stress effects corresponding to different beam theories, *International Journal of Engineering Science* **49**: 1244-1255.
[27] Bolotin V.V., 1964, *The Dynamic Stability of Elastic Systems*, Holden-Day, San Francisco.
[28] Lanhe W., Hongjun W., Daobin W., 2007, Dynamic stability analysis of FGM plates by the moving least squares differential quadrature method, *Composite Structures* **77**: 383-394.
[29] Lei X.-w., Natsuki T., Shi J.-x., Ni Q.-q., 2012, Surface effects on the vibrational frequency of double-walled carbon nanotubes using the nonlocal Timoshenko beam model, *Composites Part B: Engineering* **43**: 64-69.